Review

Cooperative control of multiple unmanned aerial systems for heavy duty carrying

Yu Herng Tan, Shupeng Lai, Kangli Wang, Ben M. Chen*

Department of Electrical & Computer Engineering, National University of Singapore, Singapore

ABSTRACT

The idea of cooperative carrying using a team of unmanned aerial vehicles (UAVs) has been viewed as a widely applicable and deployable use of unmanned multi-agent systems, yet there are very few working systems that can successfully perform such tasks due to the complexities involved. One of the primary challenges is the limited control authority of the cooperative team due to the scale of the individual agents being necessarily much smaller than the load. Here, we propose a general method that can be used to optimise the control authority of a UAV team in the case where the agents are rigidly mounted to the payload. Firstly, a tilt angle for each UAV relative to the payload is introduced to improve the yaw control of the system, as a large wide payload will invariably have a large moment of inertia in the yaw axis. The positional placement of the UAVs and the value of the tilt angle that maximises control authority was then found using an evolutionary algorithm. The optimised solution based on a case study task involves using four UAVs placed at the corner of a square payload with an inward tilt, which can be effectively controlled as a single large quadrotor. Testing results show that the full system carrying the payload can execute given trajectories autonomously with high accuracy and precision, effectively performing the task of cooperative carrying. The proposed system was successfully demonstrated at the 2017 International Micro Air Vehicles Competition.

1. Introduction

The task of load carrying has been one whereby man has benefited greatly from the use of robots. From hydraulics, pneumatics to conveyors, automation has revolutionised the way people carry and transport payloads. The use of mobile robots to transport loads is particularly interesting due to the nature of a free agent compared to the alternative of an extensive fixed delivery system. In a similar vein, aerial transportation has been predicted to be one of the major industries for unmanned aerial vehicle (UAV) applications, valued at USD 13 billion in 2016 (Mazur & Wiśniewski, 2016), and it has seen increasing involvement from major players in the technology industry. However, commercial transportation using UAVs has faced many challenges in its development, including technical complexities and legal regulations. Despite cooperation with authorities that has led to increased use of UAVs for trials in selected areas (Beene, 2017; Matonga, Nakell, & Thompson, 2017), most of these prototypes are still in their developmental stages. Different types of platforms have been investigated for their suitability for load transportation, and the advantages of each have lent themselves to different applications. Fixed wing UAVs have the advantage of long endurance and hence greater range of delivery, but require extensive grounds for take-off and landing which is not readily available under most circumstances. Unmanned helicopters, on the other hand, are able to hover and perform vertical take-off and landing (VTOL), making them more suitable for cargo transportation that requires precise load pick-ups and placements (Kuntz & Oh, 2009; Wang et al., 2014). For urban applications such as consumer deliveries, multi-rotors provide the same VTOL ability as helicopters with the added advantage of stability, positional accuracy and ability to navigate small spaces, and hence has been the primary type of vehicle used in developmental projects by companies such as DHL (Heutger & Kückelhaus, 2014) and Amazon (Gross, 2013). However, the disadvantage of multi-rotors lies in their limited endurance and range. The need to achieve a balance between the lifting and deployable range has led to the development of hybrid vehicles that are capable of both hovering and high-speed cruise flight. Prominent projects, such Google and Alphabet X's Project Wing have chosen this concept, with different platform structures being explored from an earlier tailsitter flying wing (Stewart, 2014) to the current fixed wing tiltrotor (Bort, 2017). Despite their potential, the transition between fixed wing and hover modes involves complex non-linear dynamics and the optimisation of such platforms is still a popular research topic today.

While these developmental challenges are expected of emerging technologies, the greatest limitation that will restrict the potential of aerial transportation is the amount of payload that a single vehicle can carry. The maximum payload is determined by the total lifting power of the vehicle, but the extra weight that has to be transported also affects the endurance and efficiency of the system simultaneously, with larger loads leading to shorter flight times. For many years, the steps taken to increase the maximum payload is to build bigger vehicles with greater lifting power. Although this concept works effectively on ground transport vehicles, it scales unfavourably for aerial vehicles as the weight penalty incurred to carry a larger propulsion system reinforces the need for more lifting power. Furthermore, many transport and delivery applications are targeted at usage in urban environments, and large vehicles have an inherent disadvantage in navigating congested areas. Size restrictions may also exclude the use of large vehicles entirely in many applications due to physical or legal restrictions.

Instead of a single, large agent carrying out the lifting, an alternative concept is to engage several smaller agents to cooperatively lift the load. This solution has the benefit of using smaller agents which are mechanically simpler and cheaper and thus can lead to significant cost savings compared to a single heavy-duty robot. A multi-agent system can also be reconfigured to suit the needs of the situation, making it a flexible solution for inhomogeneous tasks. Although each individual may be simpler than a single large agent, the full system consisting of all the agents involved add layers of complexities in the area of communication and control due to the need for interaction between agents. While a single agent can be responsible for its own position and attitude control, the operation of a team requires greater knowledge of each agent in the system in addition to the state of the system in the environment. The processing and dispersing of this information to each and every agent, as well as the active nature of the team, which creates additional issues in obstacle avoidance and path planning, are the challenges of implementing a multi-agent system.

While various developments have demonstrated the basic concept of inter-agent cooperation needed, there has been limited application of this to lifting heavy and large loads. Transporting large and heavy loads adds a new element to the cooperative carrying problem as the scale of each individual unit is much smaller than the payload. Although basic lifting can be achieved through using multiple agents, controlling the full system and accurate positioning becomes much more challenging as the sources of lift and hence control inputs are distributed.

There are many ways that cooperative carrying can be executed, with variables including the number of agents used, the arrangement and placement of the agents on the load and whether centralised or decentralised control is used. The nature of the full system can also vary in the type of linkage used between the payload and the vehicles. These options provide us with opportunities to resolve the aforementioned challenges through a system design process. Each configuration has its advantages and disadvantages and hence the systems could differ greatly in effectiveness and performance. As such, the general task of cooperative carrying can be seen as an optimisation problem to find the best multi-agent configuration based on objective functions usually defined by cost and effectiveness.

In this paper, we present a general optimisation method for obtaining the optimal arrangement for cooperative heavy lifting using multiple UAVs. More specifically, we propose a unique solution of using multiple UAVs for heavy duty carrying or cargo transportation in general. The main contributions of this paper is the mathematical formulation and solution of the multi-agent heavy lifting system as an optimisation problem to maximise control authority, which is the fundamental problem of such a setup. Additionally, we also propose to add an additional variable into the system's positional configuration: allowing the vehicles to be attached to the payload at an angle along the same axis so as to create a larger input acceleration for the yaw channel. The outline of this manuscript is as follows: Section 2 introduces the existing work and challenges in the area of cooperative carrying using UAVs. In Section 3, we formulate the problem mathematically by considering the case where the UAVs are rigidly mounted onto the payload. By formulating the required physical system and stability requirements as constraints and choosing a suitable objective function, the optimal configuration for a given payload can be found using an evolutionary algorithm. Section 4 details the implementation of the solution found based on a task in the 2017 International Micro Air Vehicle (IMAV) competition. The model of the system is shown in Section 5, and the control structure is presented. The performance results of the full system based on the IMAV competition task is presented and analysed in Section 6 and lastly, conclusions from the work presented and the general direction for cooperative heavy lifting are summarised in Section 7.

2. Review of existing work

The concept of multi-agent systems has been a popular research topic in recent years. Beginning with the concept of a large number of UAVs operating as a system, the coordinated control of these swarm operations were proposed in Olfati-Saber (2006). Algorithms for multi-agent path planning have been developed for many applications from basic collision avoidance (Alonso-Mora, Naegeli, Siegwart, & Beardsley, 2015) to more specific tasks like cooperative target tracking (Marsh, Calbert, Tu, Gossink, & Kwok, 2005). The capabilities of motion capture systems such as VICON and OptiTrack has allowed very accurate positioning information in enclosed spaces with little latency, which is fundamentally important for multi-agent systems. This has made the calculated trajectories implementable as accurate localisation information is essential to execute precise position control. Examples of such applications can be most commonly seen the area of formation flying (Borrelli, Keviczky, & Balas, 2004) and dynamic light displays (Kaplan, 2016a; 2016b).

Although positioning is a significant part of flying in formation, load carrying adds an additional variable to the problem. Not only does carrying weight changes the individual dynamic of each UAV, cooperative carrying means that each individual is in some way connected to each other via the payload. Problems that involve cooperation between multiple agents often use a leader-follower protocol. Chaimowicz, Sugar, Kumar, and Campos (2001) presents a software architecture for tightly coupled systems, which is defined as separate robots which have to work together in a highly coordinated manner to complete a task, that allows a flexible leader-follower arrangement. The leader is responsible for planning and dispersing trajectories to its followers, and the followers will then execute their control using the given plan. This general definition can be applied to a wide range of cooperative systems such as mobile manipulators. Cooperative carrying using UAVs are also naturally closely coupled as the nature of the setup effectively links the individual agents into a larger system.

Most existing work on cooperative carrying using UAVs are based on the use of a deformable solid link either as the payload itself or as the link between the UAVs and the payload. Although technically *deformable*, the links between the UAVs and payloads can be modelled as rigid (and not stretchable) links if they are taut at all times. The presence of a suspended load slung under a single UAV has been modelled and studied extensively, with platforms used including micro quadrotors (Weijers, 2015), standard multirotors (Mo, Geng, & Lu, 2016), unmanned helicopters (Kang, Prasad, & Johnson, 2016; Wang et al., 2015), and tiltrotors (de Almeida & Raffo, 2015; Santos & Raffo, 2016). Various strategies have been implemented to handle the dynamics of such a system. The simplest approach is to treat the force from the free-swinging load as an external disturbance, and designing a sufficiently robust attitude controller to reject this disturbance. A more sophisticated approach is to consider the load as part of the system, where the target is to find a trajectory that minimises the swing and hence improves the performance of the system. Table 1 summarises the previous work where the controller design for such a system has been

Table 1
Summary of studies involving an underslung load carried by a single UAV.

Year	Institution	Platform Type	Control strategy
2012	University of New Mexico (Cruz & Fierro, 2017; Palunko, Cruz, & Fierro, 2012)	Quadrotor	Dynamic programming
2015	National University of Singapore (Wang et al., 2015)	Helicopter	H_∞, Robust and perfect tracking (RPT)
2015	University of Twente (Weijers, 2015)	Micro quadrotor	Passivity-based control (PBC)
2016	Georgia Institute of Technology (Kang et al., 2016)	Helicopter	Adaptive neural network
2017	Norwegian University of Science and Technology (Klausen, Fossen, & Johansen, 2017)	Hexacopter	Non-linear control

Table 2
Summary of work done on cooperative carrying using multi-agent UAV teams.

Year	Institution	Platform Type	Team size	Attachment type	Vehicle weight (kg)	Payload weight (kg)	Localisation method
2010	University of Seville (Bernard, Kondak, Maza, & Ollero, 2011; Maza et al., 2010)	Helicopter	3	Flexible	12.5	4	GPS, Camera
2011	University of Pennsylvania (Michael et al., 2011)	Quadrotor	3	Flexible	0.5	0.25	VICON
2013	University of Pennsylvania (Mellinger et al., 2013)	Quadrotor	4	Rigid	0.5	1.2	VICON
2017	National University of Singapore	Quadrotor/ Hexarotor	5	Rigid	0.55/1.1	2	Laser SLAM, GPS

implemented, not including examples where only simulations were performed.

The studies on a free-swinging load carried by a UAV above forms the basic idea that is further expanded into a cooperative carrying problem where several vehicles are attached to the same payload. Implementations of multi-agent cooperative carrying with UAVs are summarised in Table 2. Michael, Fink, and Kumar (2011) models a cable-suspended payload and designs a system that is able to ensure static equilibrium using three UAVs. The work is further expanded in Fink, Michael, Kim, and Kumar (2011), where thorough motion planning of the full system is developed. The path of the full system is planned first, and the coordinated trajectories of each UAV are generated subsequently. Cooperative carrying with planning and obstacle avoidance was also implemented in Maza, Kondak, Bernard, and Ollero (2010), where a framework to incorporate multiple agents was developed. The problem was also further explored by treating the connecting cables as stretchable links in Beloti Pizetta, Brandao, and Sarcinelli-Filho (2016), where the variations in cable tensions were dealt with as a disturbance rejection problem and solved using non-linear methods.

The type of cooperative carrying discussed here is closer to the system presented in Mellinger, Shomin, Michael, and Kumar (2013), where a rigid connection is established between the UAV and the payload. This means that the UAVs and payload can be dynamically treated as a single body. While this system is much simpler to model, the moment of inertia that the vehicles involved have to overcome become significantly larger as the system has to be treated as a single large rigid body. Nevertheless, this method would be inherently more suitable than aerial towing as a heavy payload would result in a larger disturbance force that the system would need to counter.

In existing literature, the weight of the payload that can be carried by the system has rarely been discussed. In cases based on the free-hanging model where the load is treated as a disturbance to be rejected, the weight of the payload is assumed to be small. Furthermore, there is no previous work on optimising the formation of a UAV team to maximise lifting power and control authority, which are both fundamental to transporting the payload via a given trajectory. We use this aspect of cooperative carrying as a launching point for this paper with the aim of designing a UAV system that is capable of lifting and transporting heavy loads autonomously. Firstly, we adopt the same rigid mounting concept used in Mellinger et al. (2013) as the resulting system would be dynamically simpler as well as more compact in size. For a flexibly linked payload, the length of the connection is often lengthened to reduce the torque disturbances caused by the swinging of the load, which causes

the resulting system to be large and hence restrict the areas and applications where such systems can operate in. Secondly, we address the issue of control difficulties that is inevitable in such systems due to the nature of using distributed agents to cooperatively lift a heavy load. We make use of the optimisation process of the system design to overcome this challenge. Lastly, the procedure presented here can be applied to find the optimal UAV team configuration for payloads of other shapes and size, which has not been previously documented in the literature.

3. Physical solution

In this section, the design variables of a cooperative carrying UAV system are evaluated and discussed. The problem is formulated accordingly based on the constraints of the physical system and a solution is obtained using an evolutionary algorithm (EA), which is used to optimise the multiple variables in the system.

3.1. IMAV cooperative carrying task

Part of the challenge of the 2017 International Micro Air Vehicle (IMAV) competition held in Toulouse, France is to transport a given payload from a takeoff area to a specified landing point autonomously using two or more UAVs. This task was presented in both indoor and outdoor forms, challenging participants to produce a multi-agent cooperative carrying system in both GPS and GPS-denied environments. The payload to be carried is a large square wooden frame with a crossbeam as shown in Fig. 1, making the task generic and easily scalable. The frame measures 1×1 m and weighs approximately 2 kg. The symmetric payload resembles common items found in industrial warehouses such as palettes, making this specific problem defined to be suitable for generalisation and future applications.

This task can be treated as an optimisation problem with the aim of completing the specified task with the simplest or most direct system in the area of hardware structure and control. As any cooperative carrying task is essentially a system design problem, the optimal solution should also provide the greatest control authority such that any given trajectory can be closely tracked. The variables of the problem, which include the number and formation arrangement of UAVs, are discussed below.

3.1.1. Deformable link vs. rigid body

The most common solution modelled in literature is the string-based or deformable link approach, with the payload suspended from the UAV using string or cables. The minimum number of agents that can be used in this case would be two and can be extended to any number of

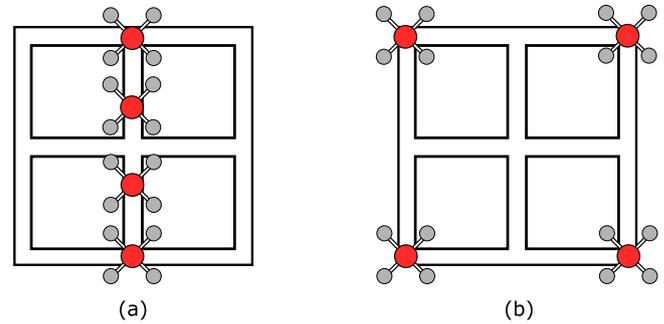Fig. 1. The payload to be carried by the UAV team.

(a)　　　　　　　　　(b)

Fig. 2. Arranging the team members in formation (a) would result in a system with less control authority in roll than formation (b).

vehicles. The difficulty then lies in the positioning and points of connection on the frame, which will affect the pose of the payload and is limited by spacing constraints of the physical system. The primary challenge of the string-based approach is the changing dynamics of the whole system to be controlled due to the nature of the joints between the UAVs and the payload and hence the inconsistent pose of the frame.

Though the string-based approach has been widely studied (Beloti Pizetta et al., 2016; Fink et al., 2011; Lee, Sreenath, & Kumar, 2013; Michael et al., 2011), the alternative solution of rigidly connecting the vehicles and the frame results in a system with a simpler dynamic model. This can be achieved either through a gripping mechanism or by manually securing the vehicles to the payload. In this case, the whole system can be treated as a single body with constant dynamics. This greatly simplifies the problem from a modelling standpoint, though the full system has to be stabilisable and controllable for this to be successfully implemented. This will be the method of attachment discussed here as it allows for greater extrapolation for systems of increasing number of agents, unlike the model of the string-based approach which becomes exponentially complicated as more UAVs are added.

3.1.2. Formation and number of UAVs

Theoretically, any number of UAVs can be mounted onto the square frame as long as the physical dimensions allow. However, it is essential that the fully mounted system is controllable for it to be a feasible solution. Although the addition of quadcopters mounted on top of a load inherently offers control authority about all axes, certain configurations will enhance the effectiveness of the control through the geometric position and hence reduce the magnitude of control input required. For example, a configuration with four UAVs along the mid-line of the square frame, as shown in Fig. 2, will have limited roll control compared to an arrangement whereby the four UAVs are placed at the corners of the frame, even though both configurations provide the same amount of total lift.

3.1.3. Yaw control

The inherent problem of the rigid attachment approach is the fact that the moment of inertia will invariably be significantly larger than the rotational acceleration each UAV can deliver. For a flat square frame, this issue is further exacerbated about the yaw axis, especially when the point loads of each UAV are placed along the outer edges. This implies that a large rotational torque will be required to control yaw. The conventional method of controlling yaw in a quadrotor is to vary the speeds of the counter-rotating propellers such that there is a net torque generated by the motors about the centre of the UAV. While the total number of counter-rotating motors is multiplied by using a team of UAVs, each motor itself is small, and hence the difference in

speeds of the counter-rotating motors needs to be large to generate sufficient torque. A large difference in rotational speeds necessarily means a loss of lift when the motors reach the saturation point, and this would significantly impair the ability of the system to maintain positional accuracy in the vertical direction.

As the conventional method to control yaw would be ineffective for this system, an alternative solution is proposed to increase the control authority of the system in the yaw axis. This can be done by tilting the corner UAVs towards the central line of symmetry of the system. By doing so, a component of thrust from each diagonally opposite UAV would be acting in the direction that creates a turning couple about the centre. By making use of the principle of moments, the total torque that can be generated by the system in the yaw axis will be much larger than the combination of individual torque from the relatively small motors. The moment generated by this component of thrust will be higher when the UAV is placed further away from the centre of the payload. However, this will also result in a higher moment of inertia in the yaw axis. The challenge is then to find the optimal placement and tilt angle such that sufficient rotational acceleration can be obtained without an excessive tilt angle which will result in a loss of lifting thrust.

3.2. Optimisation problem

Here, we formulate a general problem of obtaining the optimal arrangement of a UAV team on an arbitrary payload. The variables of this problem include the number of UAVs, the position of each UAV on the frame and the amount of tilt angle to improve yaw control. To find the optimal solution in this multi-variable problem, EA was applied based on the objective and constraints formulated below.

3.2.1. Problem formulation

The aim here is to find the optimal position and pose of the UAVs to be mounted to a 2D payload that will provide the greatest control authority in all rotational and translational directions. To simplify the problem, we will first choose the number of UAVs that will make up the team. We also fix the position of one UAV to be placed at the geometric centre of the payload. If the system is in static equilibrium, this would imply that the geometric centre would also be the centre of gravity. Placing a vehicle here would be ideal for state estimation of the whole system. This central UAV will be used primarily as a main controller, and due to its central position, would have a minimal contribution to the control effort in the rotational axes. As such, the system will be designed such that this UAV contributes only to vertical lifting and can be excluded from the rotational calculations below.

The variables to be optimised are: the 2-dimensional position points of the UAVs on the payload; and the tilt angle and direction of each UAV. As many typical payload shapes are angular and cannot be modelled directly by a continuous function, the position of the UAV will be treated as a discrete variable. The 2D payload can be mapped onto an $x - y$ plane, with the centroid of the payload at the origin. The position points will then be selected from the payload definition at

sufficiently small intervals. The tilt for each UAV is along the x-axis, and the tilt angle is defined such that a positive tilt angle in a position with a positive y value would result in a component of thrust creating a clockwise moment about the centre.

To perform the optimisation with discrete variables, the position variables are treated as single integers with each integer corresponding to a position on the frame. The integers are then mapped to the respective $x - y$ positions on the frame based on the initial integer assignment. Therefore each 2D position is represented by a single variable. This means that for a team of n UAVs, there will be n position variables and n angle variables, adding together to give a total of $2n$ variables to be found.

In order to effectively control the pose and position of the system, it is essential that the configuration provides sufficient control authority in each axis. The objective function to be maximised was formulated as the linear combination of the amount of control authority afforded by each configuration as shown in Eq. (1).

$$z = k_R \frac{\tau_y}{I_{yy}} + k_P \frac{\tau_x}{I_{xx}} + k_Y \frac{\tau_z}{I_{zz}} + k_T \frac{F_z}{m} \qquad (1)$$

The positional tracking accuracy is fundamentally dependent on the amount of control authority that the system possesses, as this dictates how quickly and effectively the system can respond. The control authority is determined by the angular acceleration about each axis and the linear acceleration in the vertical z-axis. For the three rotational axes, this is equivalent to the torque generated (τ_x, τ_y, τ_z) divided by the moment of inertia about the corresponding axis (I_{xx}, I_{yy}, I_{zz}). In the vertical direction, the linear acceleration is dependent on the mass of the system, m, and the total thrust acting in the lifting direction, $F_z = \sum_{i=1}^{n} T_{zi}$, where T_{zi} is the thrust from each individual UAV acting in the vertical z-axis. The values k_R, k_P, k_Y, k_T are scaling factors which adjust the relative importance of each component. Here, the control authority of the full system is what we aim to maximise with the arrangement of the vehicles given the physical limits of the system, hence target values cannot be directly used as there are too many unknown variables.

Constraints were then applied to ensure that the system would be physically implementable (no overlapping of UAVs) and be able to achieve static equilibrium. To ensure that the UAVs have sufficient clearance between each other, we enforce a minimum Euclidean distance of 1.1 times the diameter of the UAV, d, between each UAV position. This is formulated as

$$\sqrt{(x_i - x_j)^2 + (y_i - y_j)^2} \leq 1.1d \quad \text{for all } 1 \leq i, j \leq n, i \neq j \qquad (2)$$

To maintain static equilibrium, the net force and torque produced by the thrust of each UAV and gravity acting on it should be zero at hover state. Since the UAVs are homogenous, this means that the total sum of the position information along both axes, should be zero for equilibrium in pitch and roll. Although it is possible to equilibrate a system where there is net torque due to the 2D positions by producing counter moments from varying the thrust produced by individual motors of a single UAV, this would naturally be a sub-optimal solution and hence would not be considered here. For equilibrium in yaw, we require the torque generated by the component of thrust due to the presence of the tilt angle to be zero. These constraints are written as

$$\sum_i x_i = 0 \qquad \sum_i y_i = 0 \qquad \sum_i y_i \sin \beta_i = 0 \qquad 1 \leq i \leq n \qquad (3)$$

where β is the tilt angle. Lastly, the tilt angle allows a component of thrust to act in the $x - y$ plane to enable better yaw control at the cost of vertical thrust and hence lifting power. Although a larger amount of tilt will increase yaw control authority, the tilt cannot be too large so as to maintain sufficient lifting thrust. The last constraint is formulated as Eq. (4) to control the minimum fraction of thrust acting in the vertical direction.

$$\frac{1}{n} \sum_i \cos \beta_i > \tau \qquad 1 \leq i \leq n \qquad (4)$$

where τ is the minimum fraction of thrust allowed. This is calculated based on the thrust available from each UAV and the total weight of the system. In addition, we also limit $-\frac{\pi}{2} < \beta < \frac{\pi}{2}$ as the UAVs cannot be mounted invertedly, though under typical conditions Eq. (4) would be the limiting constraint for β.

3.2.2. Derived solution

The optimal solution for the case study was then obtained using EA based on the constraints and objective function formulated above. EA is a general method for global optimisation that is suitable for highly non-linear problems. Based on the problem formulated, EA generates a population of possible configurations and evolves the solution through the process of natural selection, much like evolution (Pétrowski & Ben-Hamida, 2017). Intuitively, four UAVs would be the minimum number needed to obtain an equally distributed and statically stable system for a square payload that has four edges, therefore the number of UAVs was selected as four. The parameters of the UAVs used in the simulation are shown in Table 3, and the optimisation parameters are shown in Table 4.

In this case, the possible positions along the frame were discrete points with increments of 0.1 m along the length of each beam ranging from -0.5 to 0.5 e.g. the centre of the frame is (0,0). Although the step size of the increment can be further reduced to increase the number of possible positions, the selected value of 0.1 m was chosen as it is sufficiently small with respect to the size of the UAV used here. Therefore, reducing the increment further would only result in greater computational requirements with minimal difference in results.

The solution converged after 466 generations, with the change in mean and best penalty function shown in Fig. 3. The optimised results are shown visually in Fig. 4. The blue circles represent the diameter of each UAV while the green arrow represents the direction and relative magnitude of the tilt angle. The results show that the optimised layout would be placing the four UAVs at the corners of the square frame with an inward tilt of 11.4 degrees. This formation is also similar to a large quadrotor, with each UAV acting as a 'propeller'. With this configuration, the problem of controlling the multiple agents in the system is simplified into a basic quadrotor control problem.

3.2.3. General payload

The process above can also be applied to payloads of other shapes. The beams that make up the payload are first discretised into position points and then the 2D shape is repositioned in the $x - y$ plane such that the centroid of the shape is at (0,0). Using the same constraints and objective functions as above, the optimal placement and tilt angles with four UAVs for two other shapes: an L-shape and a triangle are shown below in Fig. 5.

4. The combined UAV system

The optimisation process above has already found the arrangement and tilt angle for a team made up of four UAVs. To implement this, the coordinated control of each individual UAV needs to be realised. This is demonstrated here using centralised control, with the central UAV acting as the controller of the large quadrotor. The central UAV functions as a centralised controller as its pose estimation sensors are at the

Table 3
Parameters of the UAV used in the simulation based on the case study.

Diameter (tip to tip) (mm)	450
Weight (kg)	0.55
Maximum thrust	1.2

Table 4
Optimisation parameters used in the simulation.

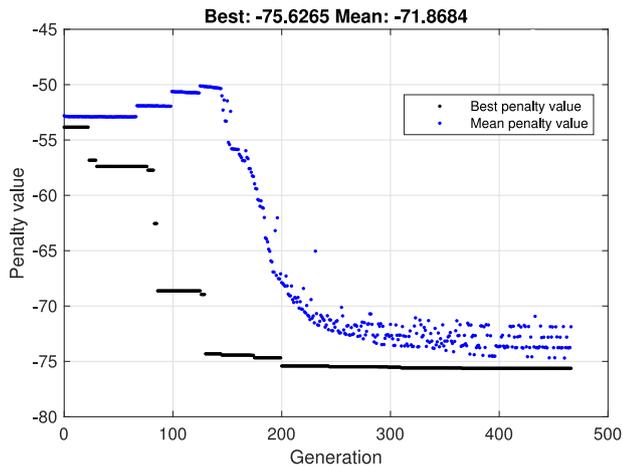|	
k_R	10
k_P	10
k_Y	200
k_T	1
m (kg)	3.7
d (m)	0.45

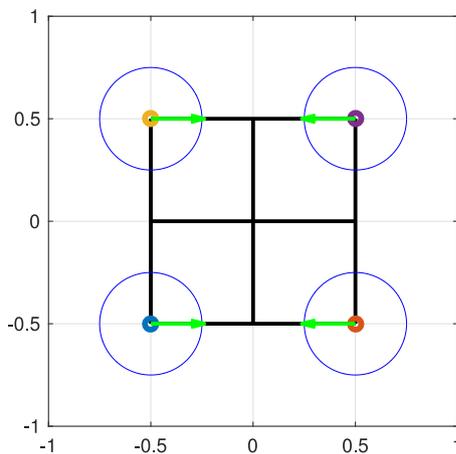**Fig. 3.** A visualisation of the solution converging over 466 generations.

Fig. 4. The results from the optimisation show that the four UAVs should be placed on the corners with an inward tilt.

centre of the system. The arrangement of the full UAV team proposed with the payload is shown in Fig. 6, and the parameters are shown in Table 5.

The UAVs used in this implementation were custom designed and built in-house at the National University of Singapore. This section discusses the physical hardware of the system proposed. The details of the UAVs and the additional subsystems uniquely required by this task are summarised below.

4.1. UAV design

For the system proposed, the choice of UAV type (i.e. quadrotor, hexarotor, octorotor etc.) does not significantly affect the overall dynamics and control considerations of the system beyond the total weight of the system and amount of lift generated. Here, two different types of vehicles are used in the team: quadrotor (Type 1) and hexarotor (Type 2). The team consists of four Type 1 UAVs placed at the

corners of the frame and a single Type 2 UAV acting as the central controller (Fig. 6). The choice of using a central hexarotor is to reduce the total lift that needs to be generated by the corner UAVs so as to minimise the weights and hence point loads acting in the corners. The four Type 1 quadrotors used are identical for simplicity and to maintain symmetry. They are based on four regular arm structures at right angles made from carbon fibre tubes. The main body of each are carbon fibre plates stacked using aluminium stand-offs. The Type 2 hexarotor uses similar construction and components as the Type 1, with a larger frame to accommodate the extra arms. The dimensions and components are summarised in Table 6 below. Each UAV carries its own flight controller and customised power distribution board. In addition, the central hexacopter carries additional navigation sensors described in Section 4.4.

4.2. Inter-agent communication

In order for the system to operate as a single large quadrotor, the individual vehicles need to be able to communicate with one another. The centralised control approach simplifies this by only requiring one-way communication from the central hexarotor to each small quadrotor. Here, a physical wire connection is utilised for high reliability and low latency communication between the central UAV and the corner UAVs. The corner UAVs can either directly control its motor speed for independent flight, or receive command signals passed from the central UAV to its motors for cooperative flight.

4.3. Mounting bracket and tilt bit

A customised bracket (Fig. 7) was designed to allow the UAVs to be securely mounted to the frame. The corner bracket aligns the robot with the two perpendicular outer edges of the frame and reusable cable ties were used to secure the whole vehicle to the payload. This design also allows the UAVs to be attached to general square frames with different dimensions.

An additional tilt bit is attached on top of the mounting bracket to implement the tilt angle required. A separate tilt bit allows the angle to be changed if necessary. Two of these tilt bits are attached to the mount and used to support the base of the UAV as shown in Fig. 7. Fig. 8 shows the full mount assembly attached to the UAV.

4.4. Positioning and localisation

To enable full autonomy of the system, the Type 2 UAV was equipped with a 4GB RAM UP Board which serves as the mission control of the full system. Various additional sensors are added for the indoor and outdoor tasks for localisation and positioning. As the Type 1 UAVs will be receiving output signals directly from the central hexacopter through signal cables, they only need to carry the basic flight control autopilot for independent operation.

For outdoor applications, the hexarotor is fitted with a GPS receiver and navigation can be done through pre-defined GPS waypoints. For indoor applications, navigation is done using 2D laser SLAM. The hexarotor carries a 20 m Hokuyo laser scanner to localise in the $x - y$ plane and uses a downward facing single beam laser for height measurement (z-positioning).

5. Modelling and control

For any unmanned system, the elements in the architecture shown in Fig. 9 is needed to execute a task autonomously. For the cooperative transportation problem here, the full system can be treated as a single vehicle as the agents are rigidly mounted and directly taking signals from the centralised controller. The higher level elements of mission management, path planning, and trajectory generation are similar to previous work done by our research group presented in Lai, Wang, and
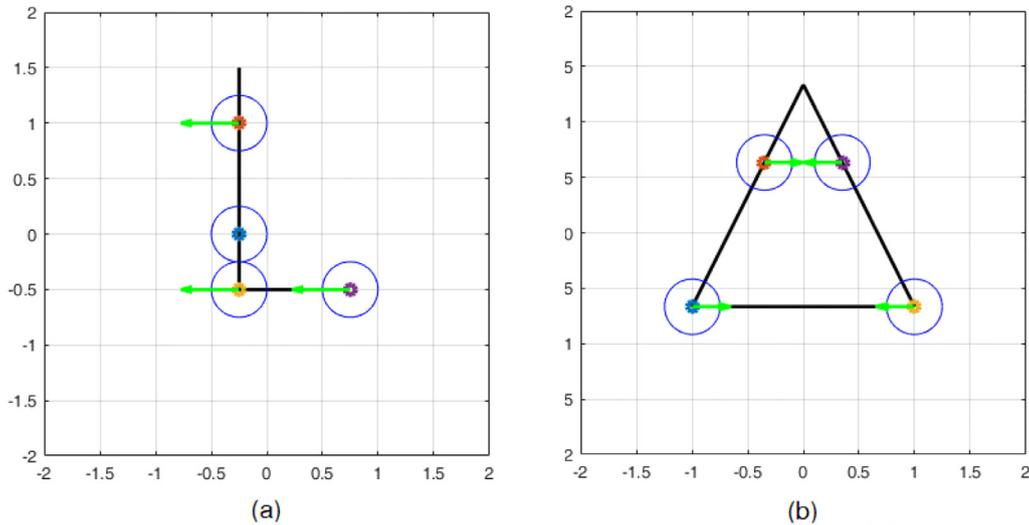
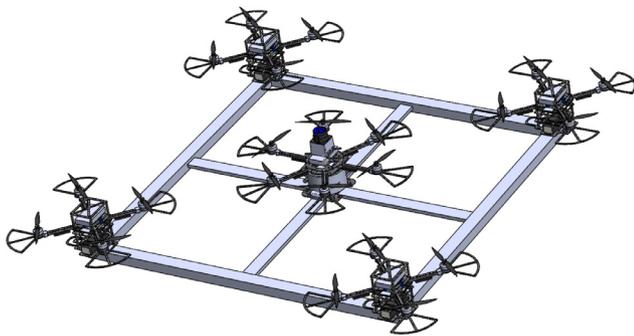**Fig. 5.** The results found for optimal placement of four UAVs on (a) an L-shape and (b) a triangular payload.

Fig. 6. CAD model of the full UAV team with the payload.

Table 5
Parameters of the full UAV system with the payload.

Maximum diameter (mm)	1864
Total weight (kg)	5.5
I_{xx} (kg/m^2)	0.79068
I_{yy} (kg/m^2)	0.79169
I_{zz} (kg/m^2)	1.55874

Table 6
Parameters of the two types of UAV used.

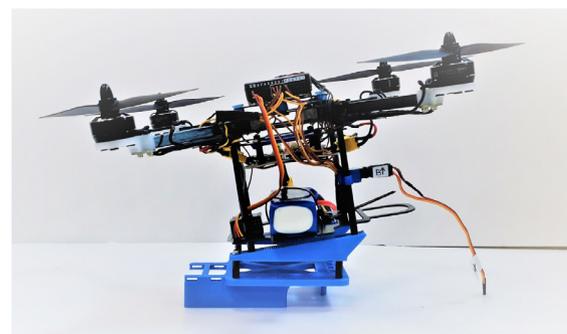| Parameter	Type 1 (Quadrotor)	Type 2 (Hexarotor)
No. of motors	4	6
Length (tip to tip) (mm)	420	600
Weight (kg)	0.55	1.1
Motor	T-Motor Air 2205-2000 KV	T-Motor Air 2205-2000 KV
Propeller (inch)	6.5 × 3.5	6.5 × 3.5
Battery	2200 mAh 3S	3400 mAh 3S

Chen (2017) and Lai, Wang, Qin, Cui, and Chen (2016). Hence, this section will focus on the inner and outer loop control of the system, which is similar to that of a typical quadrotor, with only differences in the forces used to control yaw, and different control parameters due to the larger rotational inertia.

5.1. Kinematics and modelling

The coordinate definition is shown in Fig. 10. As seen in the figure,

Fig. 7. The assembly of the mounting bracket and tilt bit attached to the bottom of all four corner UAVs.

Fig. 8. The quadrotor with the mounting bracket and tilt bit.

the local North-East-Down (NED) frame F_n is defined with X_n pointing towards the North direction, Y_n pointing towards the East direction and Z_n pointing downwards. The origin of F_n is located at the initial position of the UAV. The body frame F_b is defined as origin located at the centre of gravity of the full system, with X_b pointing towards the front of the system, Y_b pointing towards the right and Z_b pointing downwards. UAV 1 to 4 refers to the four corner UAVs, while UAV 5 is the central UAV and the corresponding sequence is shown in Fig. 10. Defining the index of the UAVs to be i, the five body frames to be attached to the five individual UAV units are then defined as F_{bi} where $i \in \{1, 2, 3, 4, 5\}$. The body frame of each single UAV is defined as x_{bi} pointing towards the front of the UAV, y_{bi} pointing towards the right side of the UAV and z_{bi} pointing downwards from the UAV. The position of the full system in
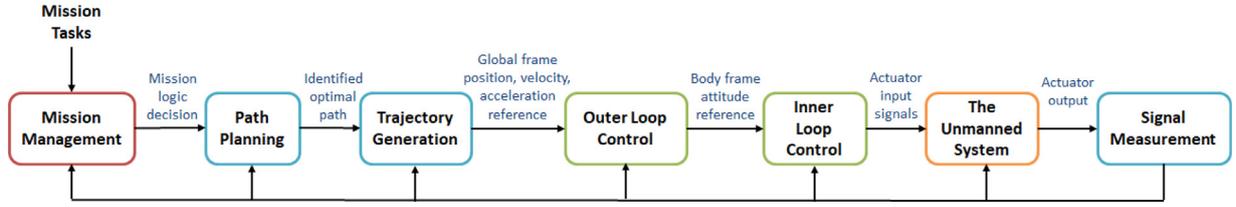
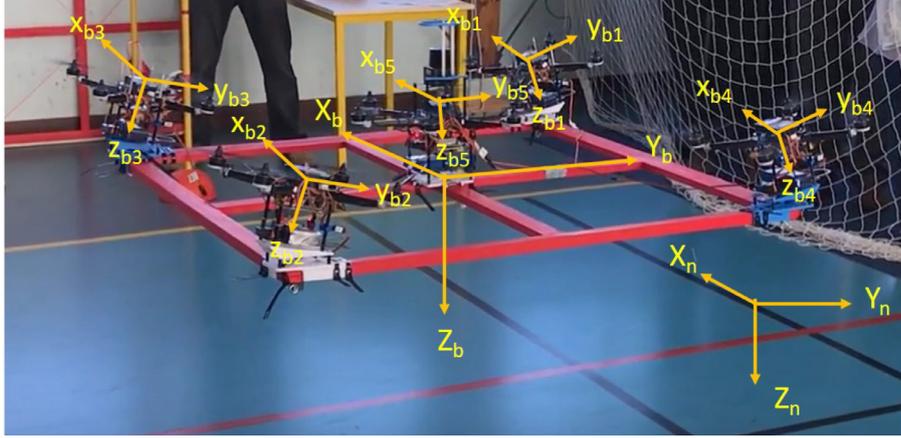**Fig. 9.** The structure of the unmanned system.

Fig. 10. The coordinate frame definition.

F_n is defined as $P_n = [x, y, z]^T$, and the orientation in F_n is defined by the Euler angles $\Theta = [\phi, \theta, \psi]^T$. The body frame velocity and body frame angular velocity are expressed as $V_b = [u, v, w]^T$ and $\omega_b = [p, q, r]^T$ respectively. The rotational and translational motions between the global and body coordinates are then given by the following navigation equations (Cai, Chen, & Lee, 2011):

$$\dot{\mathbf{P}}_\mathbf{n} = \mathbf{R}_{\mathbf{n/b}}\mathbf{V}_\mathbf{b} \tag{5}$$

$$\dot{\Theta} = \mathbf{S}^{-1}\omega_\mathbf{b} \tag{6}$$

where the rotational matrix $\mathbf{R}_{\mathbf{n/b}}$ and lumped transformation matrix $\mathbf{S}^{-1}$ are

$$\mathbf{R}_{\mathbf{n/b}} = \begin{bmatrix} c_\theta c_\psi & s_\phi s_\theta c_\psi - c_\phi s_\psi & c_\phi s_\theta c_\psi + s_\phi s_\psi \\ c_\theta s_\psi & s_\phi s_\theta s_\psi + c_\phi c_\psi & c_\phi s_\theta s_\psi - s_\phi c_\psi \\ -s_\theta & s_\phi c_\theta & c_\phi c_\theta \end{bmatrix} \tag{7}$$

$$\mathbf{S}^{-1} = \begin{bmatrix} 1 & s_\phi t_\theta & c_\phi t_\theta \\ 0 & c_\phi & -s_\phi \\ 0 & s_\phi/c_\theta & c_\phi/c_\theta \end{bmatrix} \tag{8}$$

and $s_* = \sin(*)$, $c_* = \cos(*)$ and $t_* = \tan(*)$.

The rigid body dynamics, as in the case of a standard quadrotor, can then be expressed as

$$\dot{\mathbf{V}}_\mathbf{b} = \frac{1}{m}\mathbf{F}_\mathbf{b} - \omega_\mathbf{b} \times \mathbf{V}_\mathbf{b} \tag{9}$$

$$\dot{\omega}_\mathbf{b} = \mathbf{I}^{-1}(\mathbf{M}_\mathbf{b} - \omega_\mathbf{b} \times \mathbf{I}\omega_\mathbf{b}) \tag{10}$$

where $\mathbf{F}_\mathbf{b}$ and $\mathbf{M}_\mathbf{b}$ are the net force and moments generated by the five UAVs in the frame F_b. As the system is symmetric, the inertia matrix $\mathbf{I}$ is diagonal and $I_{xx} = I_{yy}$.

$$\mathbf{I} = \begin{bmatrix} I_{xx} & 0 & 0 \\ 0 & I_{yy} & 0 \\ 0 & 0 & I_{zz} \end{bmatrix} \tag{11}$$

$\mathbf{F}_\mathbf{b}$ and $\mathbf{M}_\mathbf{b}$ can be expressed as

$$\mathbf{F}_\mathbf{b} = \sum_{i=1}^{5} \mathbf{R}_{\mathbf{b}/\mathbf{b}i}\mathbf{F}_{\mathbf{u,b}i} \tag{12}$$

$$\mathbf{M}_\mathbf{b} = \sum_{i=1}^{5} \mathbf{R}_{\mathbf{b}/\mathbf{b}i}\mathbf{M}_{\mathbf{u,b}i} \tag{13}$$

where $\mathbf{R}_{\mathbf{b}/\mathbf{b}i}$ is the rotation from F_{bi} to F_b, $\mathbf{F}_{\mathbf{u,}bi}$ and $\mathbf{M}_{\mathbf{u,}bi}$ are the force and moment generated by the ith UAV on its own body frame F_{bi} with:

$$\mathbf{R}_{\mathbf{b}/\mathbf{b}i} = \begin{bmatrix} 1 & 0 & 0 \\ 0 & \cos\beta_i & -\sin\beta_i \\ 0 & \sin\beta_i & \cos\beta_i \end{bmatrix} \tag{14}$$

For UAVs 1–4, the configuration is shown in Fig. 11, and the force and moment can be expressed as:

$$F_{\mathbf{u,b}i} = \begin{bmatrix} 0 \\ 0 \\ T_{i1} + T_{i2} + T_{i3} + T_{i4} \end{bmatrix} \tag{15}$$

$$\mathbf{M}_{\mathbf{u,b}i} = \begin{bmatrix} (-T_{i1} + T_{i2} + T_{i3} - T_{i4})\dfrac{\sqrt{2}}{2}l_{ui} \\ (T_{i1} - T_{i2} + T_{i3} - T_{i4})\dfrac{\sqrt{2}}{2}l_{ui} \\ M_{i1} + M_{i2} - M_{i3} - M_{i4} \end{bmatrix} \tag{16}$$

in which T_{ij} and M_{ij} is the lift and torque generated by the jth motor of ith UAV and l_{ui} is the distance from the motor to the centre of gravity of the ith UAV. For the fifth UAV, the hexarotor configuration is shown in Fig. 12, and the force and moment generated is:

$$F_{\mathbf{u,b5}} = \begin{bmatrix} 0 \\ 0 \\ T_{51} + T_{52} + T_{53} + T_{54} + T_{55} + T_{56} \end{bmatrix} \tag{17}$$
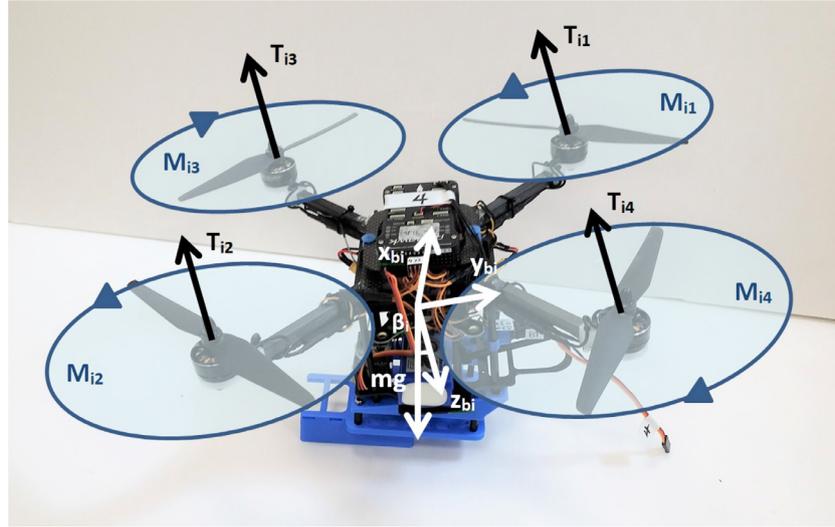
Fig. 11. The configuration of the quadrotor.

$$\mathbf{M}_{u,b5} = \begin{bmatrix} (-T_{51} - T_{53} + T_{54} + T_{56})\frac{1}{2}l_{u5} + (-T_{52} + T_{55}l_{u5})\frac{\sqrt{3}}{2}l_{u5} \\ (-T_{51} + T_{53} + T_{54} - T_{56})\frac{\sqrt{3}}{2}l_{ui} \\ M_{51} - M_{52} + M_{53} - M_{54} + M_{55} - M_{56} \end{bmatrix} \tag{18}$$

The lift and torque generated by the ij motor can be expressed as:

$$T_{ij} = K_T\omega_{ij}^2 \tag{19}$$

$$M_{ij} = K_M\omega_{ij}^2 \tag{20}$$

where ω_{ij}^2 is the rotating speed of the motor and K_T and K_M are the constant coefficient of the propeller used which can be determined experimentally.

The rotating speed of the motor ω_{ij} and the input signal δ_{ij} (scaled to [0   1]) follows the relationship (Wu, Ke, & Chen, 2016):

$$\omega_{ij}(s) = \frac{C_m}{1 + \tau_{ij}s}\delta_m(s) \tag{21}$$

where C_m is the motor rotating speed coefficient.

5.2. Inner loop control

As seen in the modelling above, there is a total of 21 motor inputs in the combined UAV system, and hence there are many ways to allocate the control input in order to control the orientation of the full system. Normally for a quadrotor or hexarotor, the roll/pitch moment is generated by the force difference of the motors and the yaw moment is generated by the torque difference of the motors. However, as a combined system, the moment of inertia in the yaw direction is far larger than the torque that can be generated by the propellers of the vehicles. As described above, an additional tilt angle for the four corner UAV allows a yawing torque to be generated from the force difference of the four corner quadrotors. To decouple the system dynamics, an intuitive way of allocating the control input is to equalise the motor speed of the four corner UAVs, i.e., $\delta_{i1} = \delta_{i2} = \delta_{i3} = \delta_{i4}$. As a result, the moment $\mathbf{M}_{u,bi} = 0$, for $i \in \{1, 2, 3, 4\}$. Moreover, varying the speed of the center hexarotor will have a minimal effect considering the central location of the hexarotor and moment of inertia of the full system. As a result, the speed input to the 6 rotors of the hexarotor are all the same. Therefore, $\mathbf{F}_b$ and $\mathbf{M}_b$ can be expressed as

$$\mathbf{F}_b = \begin{bmatrix} 0 \\ 0 \\ |T_{z1}| + |T_{z2}| + |T_{z3}| + |T_{z4}| + |T_{z5}| \end{bmatrix} + mg\begin{bmatrix} -\sin\theta \\ \sin\phi\cos\theta \\ \cos\phi\cos\theta \end{bmatrix} \tag{22}$$
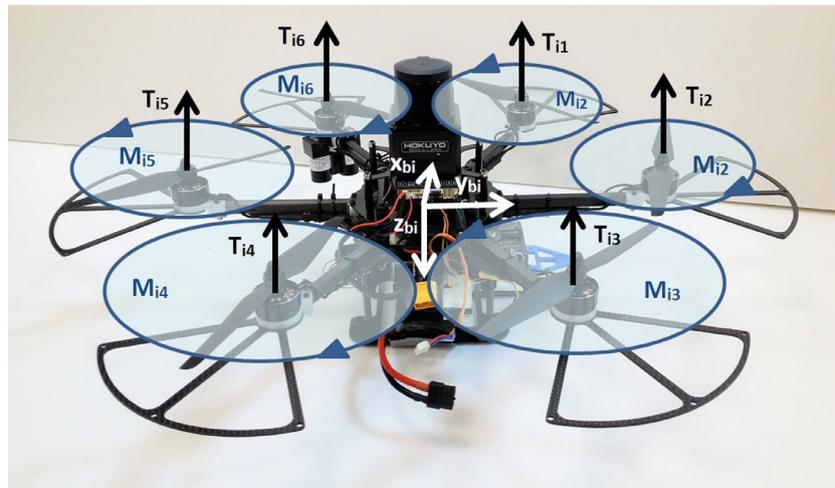

Fig. 12. The configuration of the hexarotor.

$$\mathbf{M_b} = \begin{bmatrix} \dfrac{l}{\sqrt{2}}(|T_{z2}| + |T_{z3}| - |T_{z1}| - |T_{z4}|) \\ \dfrac{l}{\sqrt{2}}(|T_{z1}| + |T_{z3}| - |T_{z2}| - |T_{z4}|) \\ (T_{y1} + T_{y2} - T_{y3} - T_{y4})\dfrac{l}{\sqrt{2}} \end{bmatrix} \tag{23}$$

Observing the above equation, it can be seen that similar to a regular quadrotor, the combined UAV is also a decoupled system in the roll, pitch, yaw and height channel. As a result, the inner loop control algorithm can be designed in roll, pitch and yaw channel independently in a similar way. The design of the roll channel is presented in this manuscript.

Since the motor propeller system has first-order dynamics as indicated in Equation (21), care has to be taken in the design of the controllers. Defining the virtual angular acceleration input of the roll dynamics to be u_x, since the angular acceleration is achieved by the rotating speed difference, the actual angular acceleration a_x is related to u_x by

$$a_x(s) = \frac{1}{1 + \tau_m(s)} u_x(s) \tag{24}$$

As such, we can define the roll channel dynamics as

$$\dot{\mathbf{x}} = \mathbf{Ax} + \mathbf{Bu} \tag{25}$$

where

$$\mathbf{x} = \begin{bmatrix} \phi & p & \int_\phi & a_x \end{bmatrix}^T,$$

which can then be explicitly written as

$$\frac{d}{dt}\mathbf{x} = \begin{bmatrix} 0 & 1 & 0 & 0 \\ 0 & 0 & 0 & 1 \\ 1 & 0 & 0 & 0 \\ 0 & 0 & 0 & -\dfrac{1}{\tau_m} \end{bmatrix}\mathbf{x} + \begin{bmatrix} 0 \\ 0 \\ 0 \\ \dfrac{1}{\tau_m} \end{bmatrix}u_x \tag{26}$$

Here, a_x is estimated by $a_x = \dot{p}$. We can then find an optimal feedback control law

$$u_x = -\mathbf{Kx} \tag{27}$$

that minimises the quadratic cost function

$$J = \int_0^\infty (\mathbf{x^T Qx} + \mathbf{u^T Ru})dt \tag{28}$$

$\mathbf{Q}$ and $\mathbf{R}$ are the positive-semidefinite and positive-definite Hermitian matrix respectively that define the relative importance of error in each state and relative cost of control signals. The LQR controller can then be designed by choosing suitable $\mathbf{Q}$ and $\mathbf{R}$ matrices and finding the matrix $\mathbf{P}$ to the Riccati equation and then the optimal feedback gain matrix can then be found as

$$\mathbf{K} = \mathbf{R^{-1}B^T P} \tag{29}$$

u_x can then be mapped to the motor speed input following Eqs. (19)–(23).

The central controller passes a single speed command to each individual UAV, hence all propellers on the same UAV rotates at the same speed. Although varying the speeds of the individual propellers on a single UAV is possible, the minimal impact of doing so does not justify the added complexity due to the difference in scale of the UAV and UAV system, which can be seen by comparing Tables 3 and 5. The roll, pitch, and yaw of the UAV system are then controlled by varying the propeller rotational speeds of each UAV. The mapping of these states to the relative propeller rotational speeds of each UAV is shown in Fig. 13.

5.3. Outer loop control

A position controller is essential for the system to successfully navigate autonomously to the target. Here, we implement robust and perfect tracking (RPT) control proposed in Chen (2000). The technique was adopted by Wang, Dong, Chen, Lee, and Phang (2012) to solve a flight formation problem. Consider a linear system characterized by

$$\begin{cases} \dot{\mathbf{x}} = \mathbf{Ax} + \mathbf{Bu} + \mathbf{Ew} \\ \mathbf{y} = \mathbf{x} \\ \mathbf{h} = \mathbf{C_2 x} + \mathbf{D_2 u} \end{cases} \tag{30}$$

where $\mathbf{x}$, $\mathbf{u}$, $\mathbf{w}$, $\mathbf{y}$, and $\mathbf{h}$ are the state, input, disturbance, measurement and controlled output, respectively. The RPT control is to design an appropriate state feedback control law such that when it is applied to the given system with any initial condition $\mathbf{x}(0)$, the resulting closed-loop system is asymptotically stable and the resulting tracking error can be made arbitrarily small in L_p sense with $p \in [1, \infty)$ provided that the disturbance $\mathbf{w} \in L_p$ with $p \in [1, \infty)$. It was proved in Chen (2000) that the RPT problem for the given system in Eq. (30) is solvable if and only if $(\mathbf{A}, \mathbf{B})$ is stabilizable and $(\mathbf{A}, \mathbf{B}, \mathbf{C_2}, \mathbf{D_2})$ is right invertible and of minimum phase.

The outer loop dynamics of the unmanned aerial system can be treated as 3 separate channels (in x, y and z direction) with no coupling effect between the channels if the closed inner loop with its controller is treated as a virtual actuator (Cai et al., 2011). Then, the dynamic equation for any one of the channels can be expressed as

$$\begin{cases} \dot{\mathbf{x}}_\mathbf{n} = \begin{bmatrix} 0 & 1 \\ 0 & 0 \end{bmatrix}\mathbf{x}_\mathbf{n} + \begin{bmatrix} 0 \\ 1 \end{bmatrix}(\mathbf{u_n} + \mathbf{w_n}) \\ \mathbf{y_n} = \mathbf{x_n} \end{cases} \tag{31}$$

where $\mathbf{x_n}$ contains the position and velocity variables, p_n and v_n, in the respective channel, and $\mathbf{w_n}$ is its acceleration disturbance due to wind gusts. An integrator should be added to ensure zero steady-state tracking error due to unmodelled bias and disturbances. We thus have the following augmented system

$$\begin{cases} \dot{\mathbf{x}}_\mathbf{a} = \begin{bmatrix} \mathbf{0} & \mathbf{1} & \mathbf{0} \\ \mathbf{0} & \mathbf{0} & \mathbf{1} \\ \mathbf{0} & \mathbf{0} & \mathbf{0} \end{bmatrix}\mathbf{x_a} + \begin{bmatrix} \mathbf{0} \\ \mathbf{0} \\ \mathbf{1} \end{bmatrix}\mathbf{u_n} + \begin{bmatrix} -1 & 0 \\ 0 & 0 \\ 0 & 1 \end{bmatrix}\begin{pmatrix} p_{n,r} \\ \mathbf{w_n} \end{pmatrix} \\ \mathbf{y_a} = \mathbf{x_a} \\ \mathbf{h_a} = \begin{bmatrix} \mathbf{1} & \mathbf{0} & \mathbf{0} \end{bmatrix}\mathbf{x_a} \end{cases} \tag{32}$$

with

$$\mathbf{x_a} = \begin{bmatrix} \int\left(p_n - p_{n,r}\right)dt \\ p_n \\ v_n \end{bmatrix} \tag{33}$$

where $p_{n,r}$ is the position reference. It is simple to verify that the subsystem from $\mathbf{u_n}$ to $\mathbf{h_a}$ is invertible and has no invariant zeros. Hence, the RPT problem for (32) is solvable. Following the procedure given in Chen (2000), the closed-form solution for the feedback gain that solves the RPT control problem can be found as

$$\mathbf{u_n} = \mathbf{F_o x_o} \tag{34}$$

with

$$\mathbf{F_o} = \begin{bmatrix} -\dfrac{k_i \omega_n^2}{\epsilon^2} & \dfrac{\omega_n^2 + 2\zeta\omega_n k_i}{\epsilon^2} & \dfrac{2\zeta\omega_n + k_i}{\epsilon} & 1 & -\dfrac{\omega_n^2 + 2\zeta\omega_n k_i}{\epsilon^2} & -\dfrac{2\zeta\omega_n + k_i}{\epsilon} \end{bmatrix} \tag{35}$$

where ϵ is the tuning parameter, k_i is a positive scalar to be selected to yield an appropriate integration action, ω_n, ζ are the natural frequency and damping ratio of the closed-loop system, respectively, and
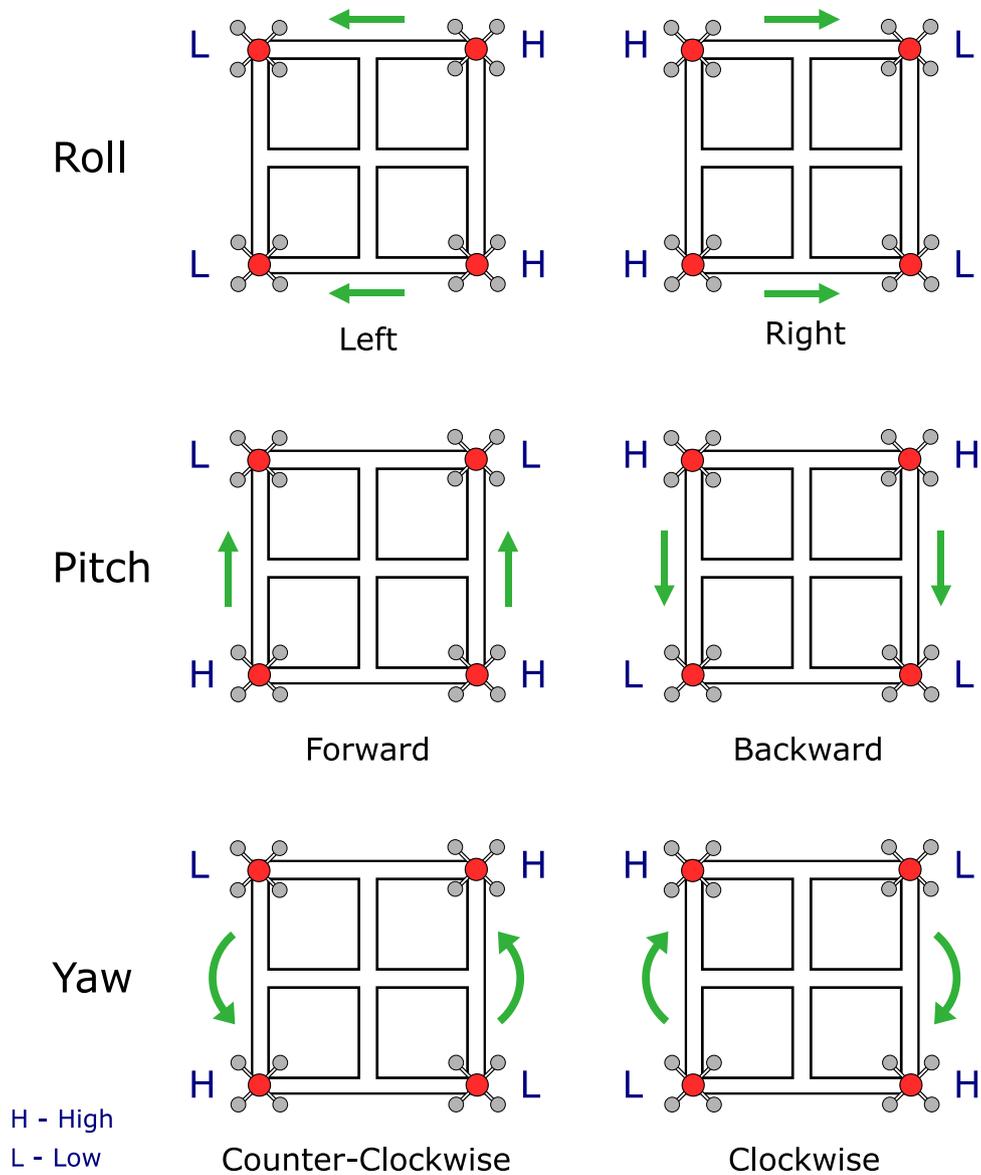
Fig. 13. The mapping of propeller speeds to each control input.

Fig. 14. Outdoor and indoor tests.

$$\mathbf{x_o} = \begin{bmatrix} \int \left(p_n - p_{n,r} \right) dt \\ p_{n,r} \\ v_{n,r} \\ a_{n,r} \\ p_n \\ v_n \end{bmatrix} \tag{36}$$

where p, v and a denote the position, velocity and acceleration and the subscript r referring to the reference signals that the system is tracking. For our combined UAV system, the gain matrix for the outer loop controller of each respective channel is given as

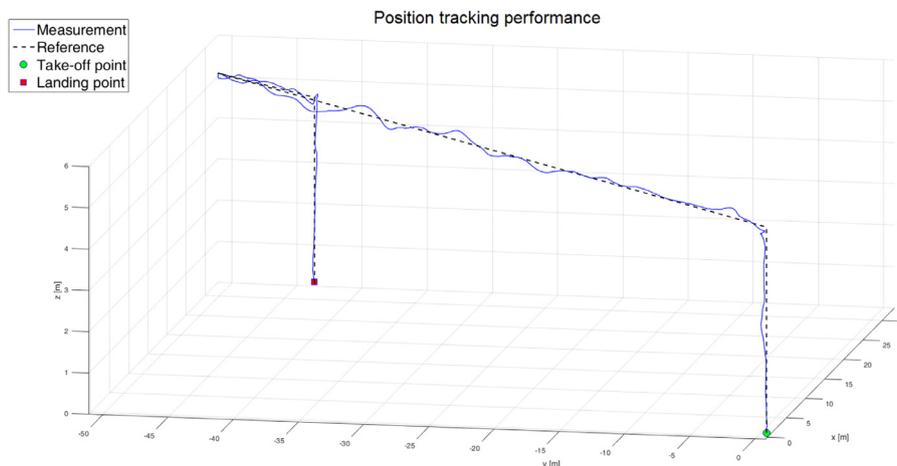$$\mathbf{F_o} = \begin{bmatrix} -0.256 & 1.088 & 1.520 & 1 & -1.088 & -1.520 \end{bmatrix} \tag{37}$$

Fig. 15. The path of the UAV team with payload compared to the reference given for the outdoor test.

6. Experiments and results

The designed system was tested and implemented in both indoor and outdoor environments (Fig. 14) at the IMAV flight competition, demonstrating the functionality of the system across a wide range of conditions. The system was able to execute the given task consistently and precisely, achieving the top awards in both the indoor and outdoor competitions. A full video recording of the system's performance in the competition can be found at this link: https://www.youtube.com/watch?v=8H19ppS_VXM.

Several trials were conducted and the results were extremely successful even in conditions of strong winds. For the outdoor mission, the team of UAVs transported the payload a distance of 50 m at a height of 5 m, moving forward at a speed of 1 m/s. After taking off, the team flies past the target landing spot by 5 m before retreating back to land. The complete flight trajectory and reference are shown in Fig. 15, and the tracking error is shown in Fig. 16. Fig. 15 shows good performance in the tracking of the given trajectory, with the path of the system being within 0.7 m of the reference at all times. The results demonstrate the strong control authority and the effective controller of the cooperative system design.

As the 2D laser SLAM provides much more precise localisation compared to GPS, the system is capable of navigating much smaller spaces when equipped with the indoor configuration. For the indoor mission, the team took off to a height of 1 m and flew forward with the

payload towards the target point 10 m ahead. Similar to the outdoor mission, it first flew past the target before retreating back and landing on the target point. Fig. 17 shows the trajectory and reference of this mission and Fig. 18 shows the tracking error.

As shown in Fig. 17, the team is again able to track the given trajectory very closely, with a deviation of less than 15 cm when the system is in forward motion. The peak in tracking error occurs when the system starts to move forward after takeoff, hence appearing as a larger error as it proceeded with the forward motion before reaching the target height vertically. The results also show that the position tracking accuracy of the system is more dependent on the localisation method, and the fact that the large system can still be effectively controlled using the conventional method with the proposed design.

The missions presented here demonstrate the position tracking accuracy of the system and general functionality of the proposed solution. Further tests showed that the current configuration carrying the payload has an endurance of around three minutes, which translates into a transportation distance of 150 m flying at a moderate speed of 1 m/s. This is considerably large, taking into account the size of the UAVs involved compared to the weight of the payload.

7. Conclusion

Cooperative carrying using UAVs is a complex optimisation problem with an infinitely large number of possible solutions. Here, we apply an optimisation based on EA to find the optimal solution for the position placement and pose of the UAVs on a known 2D payload. The dynamics of the system is simplified by utilising rigid attachment, and the requirements of the physical system form the constraints of the optimisation problem. The implementation based on the solution found provides a proof-of-concept of several aspects that can allow for greater cooperative heavy lifting using multiple UAVs. These are: firstly, the concept of mounting four UAVs in a square formation to mimic a large quadrotor and further simplify the control of the system; and secondly, adding a tilt angle to the corner quadrotors to effectively control yaw. Although the implementation used basic methods in implementing the concept by both manually hard mounting the UAVs to the payload and adding a fixed permanent tilt angle, this can be improved in further iterations with gripper mechanisms to secure the UAVs to the payloads and variable angle tilt mechanisms to optimise yaw control in different situations. Further improvements in inter-agent communications can also be made so that the transition from operating as a team to operating individually requires less manual manipulation. Nevertheless, experiments show that the system can be effectively controlled with minimal tracking error and successfully transport the given payload autonomously. The optimisation process can also be extended to
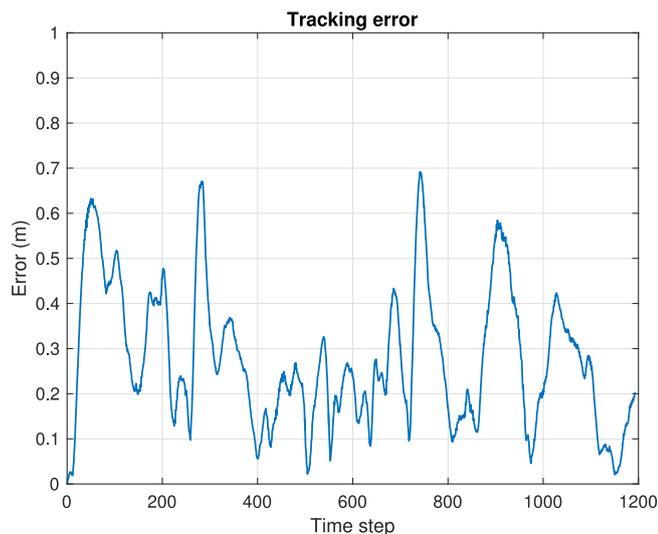

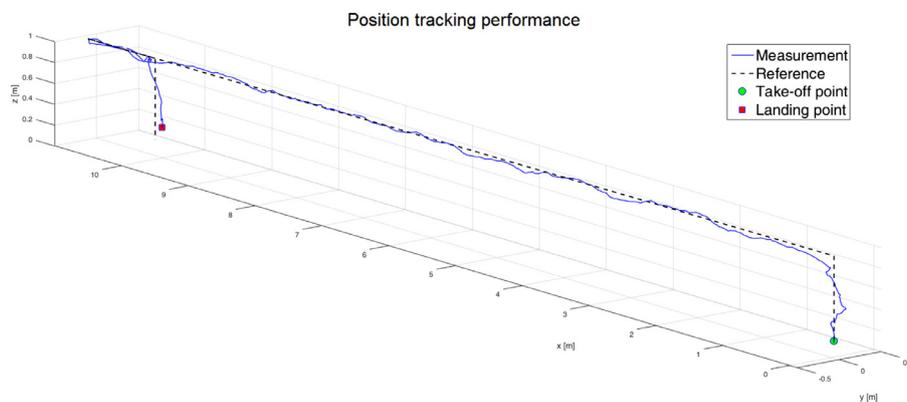Fig. 16. The tracking error of the system in the outdoor test.

Fig. 17. The path of the UAV team with payload in the indoor test.
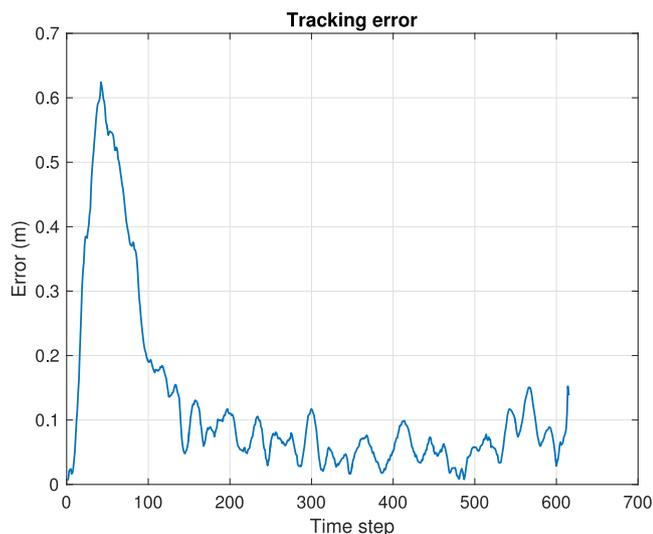

Fig. 18. The tracking error of the system in the indoor test.

payloads of different shapes and teams with a different number of UAVs.

References

Alonso-Mora, J., Naegeli, T., Siegwart, R., & Beardsley, P. (2015). Collision avoidance for aerial vehicles in multi-agent scenarios. *Autonomous Robots, 39*(1), 101–121. https://doi.org/10.1007/s10514-015-9429-0.

Beene, R. (2017). Amazon vision of deliveries by drone gets boost in FAA measure.

Beloti Pizetta, I. H., Brandao, A. S., & Sarcinelli-Filho, M. (2016). *Cooperative quadrotors carrying a suspended load. 2016 international conference on unmanned aircraft systems (ICUAS)*. IEEE1049–1055. https://doi.org/10.1109/ICUAS.2016.7502605http://ieeexplore.ieee.org/document/7502605/.

Bernard, M., Kondak, K., Maza, I., & Ollero, A. (2011). Autonomous transportation and deployment with aerial robots for search and rescue missions. *Journal of Field Robotics, 28*(6), 914–931. https://doi.org/10.1002/rob.20401.

Borrelli, F., Keviczky, T., & Balas, G. J. (2004). *Collision-free UAV formation flight using decentralized optimization and invariant sets. 2004 43rd IEEE conference on decision and control (CDC)vol. 1. 2004 43rd IEEE conference on decision and control (CDC)* IEEE1099–1104Vol.1. https://doi.org/10.1109/CDC.2004.1428839http://ieeexplore.ieee.org/document/1428839/.

Bort, J. (2017). Google's drone delivery project just shared some big news about its future.

Cai, G., Chen, B. M., & Lee, T. H. (2011). *Unmanned rotorcraft systems. Advances in Industrial Control*London: Springer Londonhttps://doi.org/10.1007/978-0-85729-635-1.

Chaimowicz, L., Sugar, T., Kumar, V., & Campos, M. F. M. (2001). *An architecture for tightly coupled multi-robot cooperation. Proceedings 2001 ICRA. IEEE international conference on robotics and automation (cat. no.01CH37164)vol. 3. Proceedings 2001 ICRA. IEEE international conference on robotics and automation (cat. no.01CH37164)* IEEE2992–2997. https://doi.org/10.1109/ROBOT.2001.933076http://ieeexplore.ieee.org/document/933076/.

Chen, B. M. (2000). *Robust and h∞ control. Communications and Control Engineering*London: Springer Londonhttps://doi.org/10.1007/978-1-4471-3653-8.

Cruz, P. J., & Fierro, R. (2017). Cable-suspended load lifting by a quadrotor UAV: Hybrid model, trajectory generation, and control. *Autonomous Robots, 41*(8), 1629–1643. https://doi.org/10.1007/s10514-017-9632-2.

de Almeida, M. M., & Raffo, G. V. (2015). Nonlinear control of a tiltrotor UAV for load transportation. *IFAC-PapersOnLine, 48*(19), 232–237. https://doi.org/10.1016/j.ifacol.2015.12.039.

Fink, J., Michael, N., Kim, S., & Kumar, V. (2011). *Planning and control for cooperative manipulation and transportation with aerial robots. Springer tracts in advanced robotics70. Springer tracts in advanced robotics* 643–659. https://doi.org/10.1007/978-3-642-19457-3_38http://link.springer.com/10.1007/978-3-642-19457-3_38.

Gross, D. (2013). Amazon's drone delivery: How would it work?

Heutger, M., & Kückelhaus, M. (2014). *Unmanned aerial vehicles in logistics. DHL Trend Research*.

Kang, K., Prasad, J. V. R., & Johnson, E. (2016). Active control of a UAV helicopter with a slung load for precision airborne cargo delivery. *Unmanned Systems, 04*(03), 213–226. https://doi.org/10.1142/S2301385016500072.

Kaplan, K. (2016a). 100 dancing drones set world record.

Kaplan, K. (2016b). 500 drones light night sky to set record.

Klausen, K., Fossen, T. I., & Johansen, T. A. (2017). Nonlinear control with swing damping of a multirotor UAV with suspended load. *Journal of Intelligent & Robotic Systems, 88*(2–4), 379–394. https://doi.org/10.1007/s10846-017-0509-6.

Kuntz, N., & Oh, P. (2009). *Autonomous cargo transport system for an unmanned aerial vehicle , using visual servoing. Systemics, Cybernetics and Informatics, 7*(6), 41–46.

Lai, S., Wang, K., & Chen, B. M. (2017). *Dynamically feasible trajectory generation method for quadrotor unmanned vehicles with state constraints. 2017 36th chinese control conference (CCC)*. IEEE6252–6257. https://doi.org/10.1007/s11768-016-6007-8http://ieeexplore.ieee.org/document/8028351/.

Lai, S., Wang, K., Qin, H., Cui, J. Q., & Chen, B. M. (2016). A robust online path planning approach in cluttered environments for micro rotorcraft drones. *Control Theory and Technology, 14*(1), 83–96. https://doi.org/10.1007/s11768-016-6007-8.

Lee, T., Sreenath, K., & Kumar, V. (2013). *Geometric control of cooperating multiple quadrotor UAVs with a suspended payload. 52nd IEEE conference on decision and control*. IEEE5510–5515. https://doi.org/10.1109/CDC.2013.6760757http://ieeexplore.ieee.org/document/6760757/.

Marsh, L., Calbert, G., Tu, J., Gossink, D., & Kwok, H. (2005). *Multi-agent UAV path planning. MODSIM05 - International Congress on Modelling and Simulation: Advances and Applications for Management and Decision Making, Proceedings, 2188–2194*.

Matonga, D., Nakell, P., & Thompson, G. (2017). Africa's first humanitarian drone testing corridor launched in Malawi by government and UNICEF.

Maza, I., Kondak, K., Bernard, M., & Ollero, A. (2010). Multi-UAV cooperation and control for load transportation and deployment. *Journal of Intelligent and Robotic Systems, 57*(1–4), 417–449. https://doi.org/10.1007/s10846-009-9352-8.

Mazur, M., & Wiśniewski, A. (2016). *Clarity from above: PwC global report on the commercial applications of drone technologyTechnical Report*.

Mellinger, D., Shomin, M., Michael, N., & Kumar, V. (2013). *Cooperative grasping and transport using multiple quadrotors. Distributed autonomous robotics systemsvol. 83. Distributed autonomous robotics systems* 545–558. https://doi.org/10.1007/978-3-642-32723-0_39http://link.springer.com/10.1007/978-3-642-32723-0_39.

Michael, N., Fink, J., & Kumar, V. (2011). Cooperative manipulation and transportation with aerial robots. *Autonomous Robots, 30*(1), 73–86. https://doi.org/10.1007/s10514-010-9205-0.

Mo, R., Geng, Q., & Lu, X. (2016). *Study on control method of a rotor UAV transportation with slung-load. 2016 35th chinese control conference (CCC)*. IEEE3274–3279. https://doi.org/10.1109/ChiCC.2016.7553861http://ieeexplore.ieee.org/document/7553861/.

Olfati-Saber, R. (2006). Flocking for multi-agent dynamic systems: Algorithms and theory. *IEEE Transactions on Automatic Control, 51*(3), 401–420. https://doi.org/10.1109/TAC.2005.864190.

Palunko, I., Cruz, P., & Fierro, R. (2012). Agile load transportation: Safe and efficient load manipulation with aerial robots. *IEEE Robotics & Automation Magazine, 19*(3), 69–79. https://doi.org/10.1109/MRA.2012.2205617.

Pétrowski, A., & Ben-Hamida, S. (2017). *Evolutionary algorithms. Hoboken, NJ, USA: John Wiley & Sons, Inc*https://doi.org/10.1002/9781119136378.

Santos, M. A., & Raffo, G. V. (2016). *Path tracking model predictive control of a tilt-rotor*

UAV carrying a suspended load. 2016 IEEE 19th international conference on intelligent transportation systems (ITSC). IEEE1458–1463. https://doi.org/10.1109/ITSC.2016.7795749http://ieeexplore.ieee.org/document/7795749/.

Stewart, J. (2014). Google tests drone deliveries in project wing trials.

Wang, B., Dong, X., Chen, B. M., Lee, T. H., & Phang, S. K. (2012). *Formation flight of unmanned rotorcraft based on robust and perfect tracking approach. 2012 american control conference (ACC)*. IEEE3284–3290. https://doi.org/10.1109/ACC.2012.6315049http://ieeexplore.ieee.org/document/6315049/.

Wang, F., Liu, P., Zhao, S., Chen, B. M., Phang, S. K., Lai, S., et al. (2014). *Guidance, navigation and control of an unmanned helicopter for automatic cargo transportation. Proceedings of the 33rd chinese control conference*. IEEE1013–1020. https://doi.org/10.1109/ChiCC.2014.6896766http://ieeexplore.ieee.org/lpdocs/epic03/wrapper.htm?arnumber=6896766.

Wang, F., Liu, P., Zhao, S., Chen, B. M., Phang, S. K., Lai, S., et al. (2015). Development of an unmanned helicopter for vertical replenishment. *Unmanned Systems, 03*(01), 63–87. https://doi.org/10.1142/S2301385015500053.

Weijers, M. (2015). *Minimum swing control of a UAV with a cable suspended load*. University of Twente Ph.D. thesis.

Wu, L., Ke, Y., & Chen, B. M. (2016). *Systematic modeling of rotor dynamics for small unmanned aerial vehicles. International micro air vehicles competition and conference, Beijing, China*284–290.